

# Global observations of substorm injection region evolution: 27 August 2001

E. Spanswick<sup>1</sup>, E. Donovan<sup>1</sup>, W. Liu<sup>2</sup>, J. Liang<sup>2</sup>, J. B. Blake<sup>3</sup>, G. Reeves<sup>4</sup>, R. Friedel<sup>4</sup>, B. Jackel<sup>1</sup>, C. Cully<sup>5</sup>, and A. Weatherwax<sup>6</sup>

<sup>1</sup>University of Calgary, Calgary, Alberta, Canada

<sup>2</sup>Canadian Space Agency, St.-Hubert, Quebec, Canada

<sup>3</sup>Aero Space, Los Angeles, California, USA

<sup>4</sup>Los Alamos National Laboratory, Los Alamos, NM, USA

<sup>5</sup>Swedish Institute of Space Physics, Uppsala, Sweden

<sup>6</sup>Siena Collage, New York, USA

Received: 21 October 2008 – Revised: 5 March 2009 – Accepted: 5 March 2009 – Published: 4 May 2009

**Abstract.** We present riometer and in situ observations of a substorm electron injection on 27 August 2001. The event is seen at more than 20 separate locations (including ground stations and 6 satellites: Cluster, Polar, Chandra, and 3 Los Alamos National Laboratory (LANL) spacecraft). The injection is observed to be dispersionless at 12 of these locations. Combining these observations with information from the GOES-8 geosynchronous satellite we argue that the injection initiated near geosynchronous orbit and expanded poleward (tailward) and equatorward (earthward) afterward. Further, the injection began several minutes after the reconnection identified in the Cluster data, thus providing concrete evidence that, in at least some events, near-Earth reconnection has little if any ionospheric signature.

**Keywords.** Magnetospheric physics (Energetic particles, precipitating; Magnetotail; Storms and substorms)

## 1 Introduction

Substorm associated enhancement of the plasma sheet high energy particle population (an injection) accompanies most expansive phase onsets. The sparse nature of satellite measurements in the magnetotail has meant there are few observations of the onset and subsequent evolution of this phenomenon, and to date there has not been an observationally complete picture of injection evolution. Recent studies based on ground-based riometers have shown that it is possible to

identify this key substorm signature from the ground (Spanswick et al., 2007). With a suitably dense and extensive network of riometers we can identify the starting location of the injection and follow its evolution, as projected along magnetic field lines into the ionosphere. We do not, however, have a way to interpret these observations in terms of precise magnetospheric location. The addition of direct in situ observations to the ionospheric picture can provide a reality check and allow us to infer information about the magnetospheric location of the injection region, something that is still debated. In this paper we present the first observations of an evolving injection region from the ground, accompanied by in situ measurements from Polar, Cluster, GOES, Los Alamos National Laboratory (LANL), and Chandra.

The event occurred on 27 August 2001 and began with reconnection in the central plasma sheet ( $X \sim -18 R_E$ ) at approximately 04:01 UT as inferred from Cluster data (Baker et al., 2002). Figure 1 is a similar plot to that shown in Baker et al. (2002) and presents evidence for reconnection at Cluster. Data in Fig. 1 is plotted in a GSM-like event-specific coordinate system determined using multipoint techniques and designed to minimize errors from misalignments between the current sheet and the GSM system. The  $y$  component is along the mean current direction (Robert et al., 2000) in the quiet interval 03:47–03:50 UT;  $z$  is normal to  $y$  and as near as possible to the maximum gradient (Harvey et al., 2000) in the magnetic field strength, and  $x$  completes the right-hand system. For this particular event, the system is within 16 degrees of GSM; for similar plots in GSM, see Baker et al. (2002).

Shortly after 04:01 UT, there was a negative excursion in  $B_z$  at all satellites accompanied by tailward perpendicular flow at near-Alfvénic speeds, consistent with reconnection



Correspondence to: E. Spanswick  
(elspansw@ucalgary.ca)

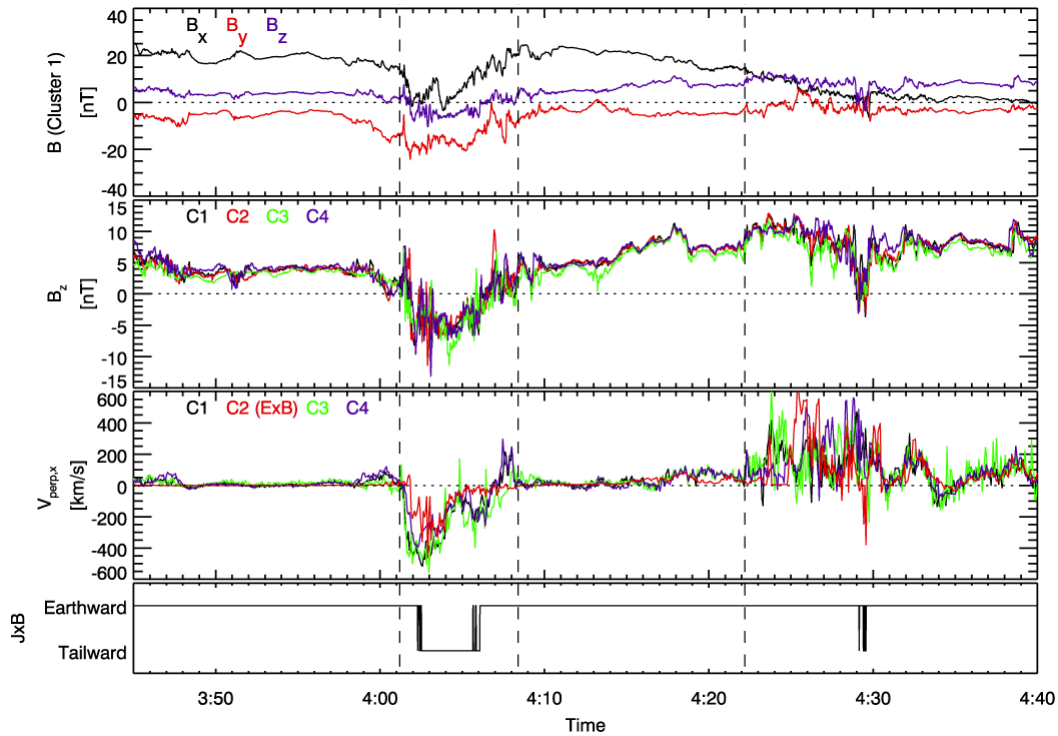


**Fig. 1.** (a) Magnetic field measured at Cluster 1 in event-specific coordinates. (b) z-component (event-specific coordinates) of the magnetic field at all 4 satellites. (c) Velocities perpendicular to the magnetic field. Since data are not available from the ion spectrometer on Cluster 2, the red line shows instead the  $\mathbf{E} \times \mathbf{B}$  velocity from the electric and magnetic field instruments. For the other satellites, the  $\mathbf{E} \times \mathbf{B}$  velocities agree well with the perpendicular velocities shown. (d) Sense of the  $\mathbf{J} \times \mathbf{B}$  vector (Earthward/tailward).

Earthward of the satellite location at  $19 R_E$  downtail. The simultaneous enhancement in  $B_y$  is consistent with the formation of a flux rope, while the drop in  $B_x$  is the result of undulations in the sheet. These undulations caused the spacecraft return to the lobes at 04:08. When the satellites once again approached the central plasma sheet after 04:22, they encountered strong Earthward flow consistent with the X-line having retreated to a more tailward location.

The main evidence for a change in topology comes from the change of sign of  $B_z$  associated simultaneously with the observation of the first ion jet. A closely related but more robust and frame-independent measure is the  $\mathbf{J} \times \mathbf{B}$  vector (panel d), which is typically oriented Earthward near the center of the sheet, consistent of Earth-connected field lines. At 04:02,  $\mathbf{J} \times \mathbf{B}$  changed from an Earthward to a tailward orientation, indicating field lines that were not connected to the Earth. Based on the above evidence, reconnection initiated inside of  $19 R_E$  prior to 04:01:30 UT.

Auroral onset associated with this event occurred approximately seven minutes later at 04:08:19 UT, as identified from IMAGE WIC (see Fig. 2 of Baker et al., 2002). Initiation of the injection and the subsequent evolution of the injection region in the inner magnetosphere was simulated by Li et al. (2003). In this “convection-surge” type simulation, the injection region forms in the mid-tail (at the observed loca-

tion of reconnection, in this case  $X \sim -18 R_E$ ) and develops in such a way that it moves Earthward, increasing the particle energy up to those observed at geosynchronous orbit. A transient magnetic field pulse, which propagates Earthward from the reconnection site, reverses the local magnetic field gradient and brings particles into the inner Central Plasma Sheet (CPS) without separation due to energy and species dependent drifts. To agree with the observations of Baker et al. (2002), the pulse takes approximately 8 min to propagate from  $-18 R_E$  to  $-6.6 R_E$ , and places the onset of injection in the geosynchronous L-shell at approximately 04:08 (Li et al., 2003).

Blake et al. (2005) examined the high-energy electron signatures during this period using Cluster, Polar and Chandra data. In that study it was noted that the onset of dispersionless injection in geosynchronous orbit (inferred from Li et al., 2003) was 04:08 UT, twelve minutes prior to the injection seen at Polar, Cluster and Chandra. The authors use this fact to argue against a localized initiation of the injection region in this event.

In this paper, we build on the work of Blake et al. (2005) and add ground-based riometer observations of the high-energy electron population to the overall picture of injection region evolution. The event of 27 August 2001 was perfectly situated over the heart of the Canadian GeoSpace Monitoring

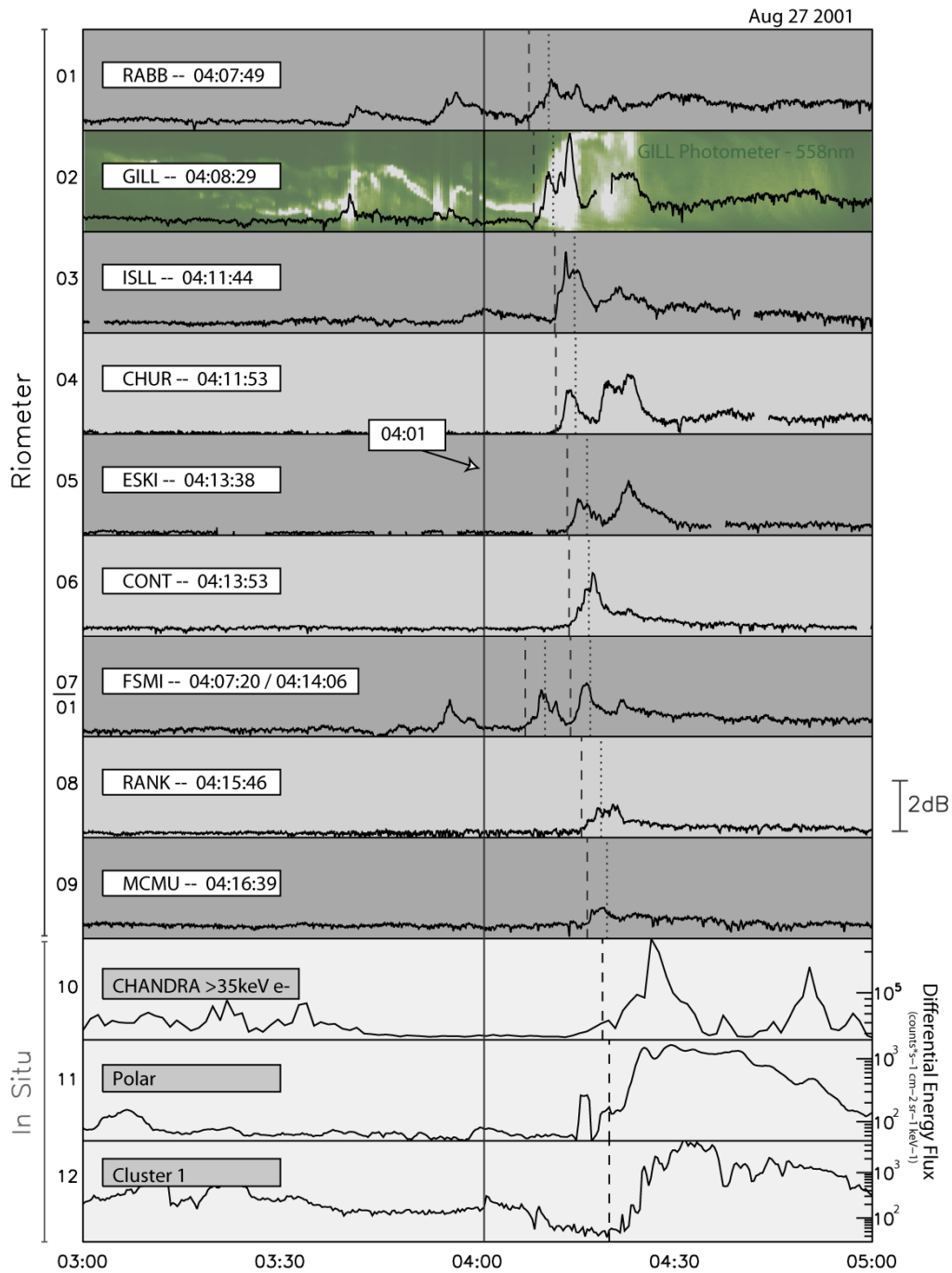


**Fig. 2.** Data and onset times for the 12 point observations of the dispersionless electron injection on 27 August 2001. Panels are plotted in order of onset time, with the earliest onset shown at the top. Panels 1–9 are riometer absorption (in dB) from CGSM riometers, an increase in absorption is a positive deviation of the line. Gillam Meridian Scanning Photometer data from the 557.7 nm channel is shown in the background of panel 2. High-energy electron measurements from Chandra, Polar and Cluster 1 are shown in panels 10, 11, and 12, respectively.

(CGSM) riometer array, allowing us to identify the location of onset and follow the ionospheric projection of the injection region throughout the substorm expansive phase. We will show that the injection did, in fact, start in a localized

region, which we interpret as being near geosynchronous orbit. This injection initiated nearly 8 min after the onset of magnetic reconnection in the mid-tail. Further, there was no discernable signature of the reconnection, nor the fast flows

that were undoubtedly associated with it, in the ionosphere during that time.

## 2 Instrumentation

We use data from the CGSM riometer network consisting of 13 single/wide beam riometers distributed across central northern Canada operating at 30 MHz and producing data at a 5 s cadence. To extend our longitudinal coverage, we also use data from the Sodankylä Geophysical Observatory riometers in Scandinavia, and the South Pole and McMurdo Station Antarctic riometers. The onset was close to the Churchill meridian in Canada, and we use optical data from the CGSM Gillam Meridian Scanning Photometer (MSP) to identify pseudo-breakup activity.

We also use high-energy electron data from Polar, Chandra and Cluster 1 previously published in Blake et al. (2005). Each of Polar and the four Cluster spacecraft carry an Imaging Electron Sensor (IES) which measures electron flux in the energy range  $\sim 35$  keV to  $>400$  keV (Blake et al., 1995; Wilken et al., 1997). From the Chandra spacecraft we use the  $>30$  keV electron channel of the Electron Proton Helium Instrument (EPHIN). See Blake et al. (2005) for the locations of the spacecraft.

## 3 Observations

Our primary data source for this study is the CGSM riometer array. Riometers remote sense enhanced ionization in the upper atmosphere due to high-energy electron precipitation, empirically found to be the  $>30$  keV electron population (see for example, Baker et al., 1981). Provided certain conditions are met, namely that the equatorial flux levels exceed the Kennel Petschek limit for strong pitch angle scattering (Kennel and Petschek, 1966), riometer absorption measured at the footpoint of an in situ satellite will mimic the  $>30$  keV electron flux (Baker et al., 1981). The connection of riometer absorption to the total electron flux above 30 keV allows us to use riometers to remote sense the evolution of the high-energy electron population for events in which the flux level is expected to be relatively high, in this case a substorm injection. During the substorm event of 27 August 2001, nine riometers across Canada displayed signatures that meet the criterion for dispersionless electron injections described by Spanswick et al. (2007). Riometer classification of “dispersionless” requires that the rise in the signature be less than three minutes and that the absorption is enhanced for at least 15 min. Panels one through nine of Fig. 2 are riometer absorption and injection onset times from the relevant CGSM riometers for this event. Panels are plotted in the order of injection onset time, with the earliest onset shown in the top panel. The injection onset ( $T_0$ ) is marked with a dashed line and  $T_0+3$  min is indicated with a dotted line. We note that for the CONT riometer the onset is slightly outside (10 s) of three

minutes. This corresponds to only two data points, so we will include CONT as a dispersionless injection for this study. We also include data from the Gillam MSP (the 558 nm channel is shown in the same panel as the GILL riometer) and in situ electron data previously presented in Blake et al. (2005) from Cluster 1, Polar and Chandra. The onset times from the Blake et al. study are shown as dashed lines.

Three riometers (RABB, GILL and FSMI) show absorption prior to what we would classify as the onset of dispersionless injection. We associate this absorption with the pseudo breakups that were noted by Baker et al. (2002) and that are evident in the GILL MSP data. There are two pseudo-breakups, and in the case of the Fort Smith riometer (FSMI #7/1 in Fig. 2) it is difficult to argue conclusively that the riometer absorption is not connected with the preceding pseudo-breakup. For this reason, we do not include Fort Smith in the data used to track the spatio-temporal evolution of the injection region.

Figure 3 shows the locations of the ground-based stations numbered according to the order in which they observed the dispersionless injection. The injection is first seen at Rabbit Lake (RABB) at approximately 04:08 UT, the same time reported by Baker et al. (2002) for the auroral onset in global auroral images from the IMAGE spacecraft. Within 40s the injection expanded east to GILL and we see the appearance of absorption “spikes” (Hargreaves et al., 1979; Spanswick et al., 2005). At approximately the same time (04:09) GOES-8 observed a dipolarization at GSM-Z $\sim 1 R_E$  in geosynchronous orbit (data not shown). The footpoint of GOES-8 is shown in Fig. 3. After 04:09, the injection region expands both east-west and north-south to cover much of the NORSTAR riometer array.

Within the context of the Blake et al. (2005) study, the riometer measurements presented here provide a finer scale observation of the expansion of the injection region between the satellite locations. For this event, the NORSTAR array falls exactly in the longitudinal gap between Polar, Cluster, and Chandra. Polar and Cluster are to the East of the NORSTAR array and Chandra to the West. Blake et al. noted that onset of the injection seen at geosynchronous orbit (04:08 as modelled by Li et al., 2003) was 12 min prior to the onset of injection at the three satellites in the tail. Using the ground-based measurements we can confirm the onset of injection at 04:08 (RABB), and track the expansion of the injection to the approximate longitude of the satellites (see Fig. 3). We do not attempt to map the locations of the satellites in the mid-tail since they will inevitably be wrong during the dipolarization process.

In addition to the dispersionless injection observations, another 7 riometers saw a distinct rise in absorption which cannot be conclusively classified as dispersionless. As the “rise time” of the signature increases the likelihood that it is associated with a dispersionless injection decreases (Spanswick et al., 2007), so we treat this signature as an indicator of dispersed injection. Although we do not show the data from the

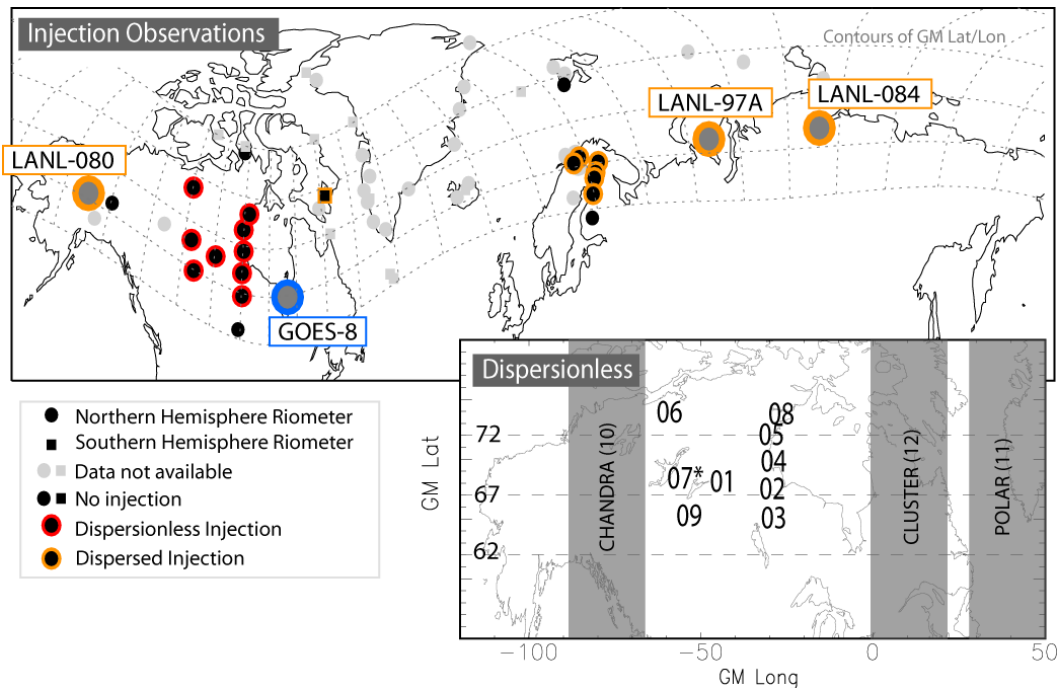


**Fig. 3.** Top: locations of all riometers used in this study along with the mappings of GOES-8 and three LANL spacecraft. Stations are colour coded according to the type of injection observed (see legend in bottom left). Bottom-Right: timing of the injection seen in the NORSTAR array. Stations are numbered according to Fig. 2, the order in which a dispersionless injection was observed. We also show the GM meridians for Chandra, Polar and Cluster (note: these are not mapped using a field line model).

dispersed riometer injections, the timing is consistent with an eastward travelling (gradient/curvature drifting) electron population. This electron population was also observed by three LANL satellites located on the dayside. The locations of the dispersed injection signatures are also shown in Fig. 3. In total, there are 22 observations of the energetic electron population for this event.

#### 4 Discussion

Using ground-based tools we can monitor the 2-D ionospheric projection of the dispersionless electron injection region (Spanswick et al., 2007). We have applied this technique to a substorm (27 August 2001) in which there was substantial in situ support data. For this event, we first observe the electron injection at a single station (RABB) at approximately 04:08 UT. The injection expands quickly to GILL and a dipolarization is observed at GOES-8 at roughly the same time. The injection observed at GILL is the closest signature in time to that of the GOES-8 dipolarization. Since we find no evidence of an injection earlier and poleward of these stations, the dipolarization/injection was underway in the inner magnetosphere at 04:09 but not at distances further down-tail. We conclude that the injection/dipolarization initiated somewhere to the west of GOES-8 near the equatorial mapping of RABB at approximately 04:08. Further,

the injection must have initiated in a region smaller than the separation between riometers and expanded, at least initially, azimuthally. Since the station immediately to the west of RABB is Fort Smith (FSMI) we cannot comment on the westward expansion of the injection region. It is interesting to note that only FSMI, RABB and GILL observed pseudo-breakup activity prior to onset. These are the east-west aligned chain associated with the initial expansion of the injection region.

Baker et al. (2002) reported reconnection in the mid-tail at approximately 04:01 for this event (this time is shown as a solid line in Fig. 2). We find no evidence of riometer activity associated specifically with this time, although as discussed above Cluster may be outside of the field of view of the riometer array. We also see no evidence of an earthward (equatorward) evolving absorption signature, only an explosive onset of injection which we can conclusively place in the inner magnetosphere. This, along with the Blake et al. results, point to an expansion of the injection region from the inner magnetosphere down-tail and not the reverse. This is contrary to the scenario modelled by Li et al. (2003), wherein injection initiates in the mid-tail (at the reconnection site) and evolves radially inwards resulting in the injection as typically observed in the inner magnetosphere. While we do not propose an alternate mechanism for the injection, we assert that the scenario evoked by Li et al. (2003) cannot explain the

comprehensive energetic electron measurements presented here. These observations are better explained by the injection model of Zaharia et al. (2000). In the Zaharia et al. model, the source region of injection particles was found to be closer to the Earth, in a region around 9Re. However, this model still does not account for the tailward propagation of the injection boundary. We speculate that this feature may relate the expansion of the injection region to the tailward propagation of dipolarization (see for example, Baumjohann et al., 2000). We also speculate that reconnection and the associated earthward flows may not have a detectable ionospheric signature in this event. This differs from events presented by Henderson et al. (2002) in which North-South auroral structures within a double oval configuration were clearly associated with earthward flow bursts in the CPS. How and why the ionospheric signature of mid-tail reconnection (and its associated earthward flows) can vary on an event-to-event basis is unclear.

The presence of absorption spikes during substorms has been well documented (Hargreaves et al., 1979; Hargreaves et al., 1997; Spanswick et al., 2006). The location of these spikes within the dispersionless injection region has previously been modelled by Liang et al. (2007). In that study, spikes were shown to be a direct consequence of drift loss/leakage of electrons from a dipolarizing flux tube. This causes a characteristically short timescale rise and fall in riometer absorption (the “spike”) which is significantly shorter than the normal decay driven by precipitation. Typically the conditions for absorption spikes are met on the western edge of the injection region, in this event that is not the case, which may suggest a “successively emerging dipolarization structure toward the morning sector” (Liang et al., 2007). In this model, each spike is a sudden rise indicative of a physical “jump” in injection region location and the decay results for a drifting population without further sources. In a continuous motion/expansion of the injection region, these types of signatures would not be expected since the source population is continuous throughout the motion/expansion. The two successive peaks shown in the GILL riometer (Fig. 2) are indicative of this type of multi-stage evolution of the expansion of the injection. The evolution was not uniform but likely in a stepwise leap-frog fashion. For example, the second intensification appeared as “spike” at GILL, implying that the GILL station might have located near the western edge of newly developed injection region, but clearly the fine scale structure of the injection region is not resolved with the grid of current ground stations.

## 5 Conclusions

We have used the CGSM array of 13 riometers to locate the initiation of a dispersionless electron injection region and track its evolution for a single event on 27 August 2001. Based on these observations we assert that in this event the

injection region initiates in the inner magnetosphere near geosynchronous orbit and expands radially outward. Further, the injection region initiates after the onset of reconnection in the mid-tail and is not a result of the dipolarization pulse that is the basis of Li et al. (2003) models of the spatio-temporal evolution of the dispersionless injection. It is clear from these observations, although it is not a surprise, that the injection is part of a multi-stage process. In this case, reconnection is clearly underway for at least 7 min prior to the initiation of injection. It is likely that the reconnection initiated a sequence of events that leads ultimately to the onset of injection which, based on the MSP data corresponds to the auroral onset. Given that the reconnection in this case has no obvious ionospheric signature, these observations indicate that ionospheric observations alone cannot be used to argue that an auroral onset was not preceded by mid-tail reconnection (see e.g., Donovan et al., 2008).

*Acknowledgements.* The Canadian Space Agency provides financial and operational support for the CGSM riometer array and the Meridian Scanning Photometer at GILL. We acknowledge the efforts of Don Wallis and Fokke Creutzberg in maintaining these instruments. Siena College gratefully acknowledges support from NSF grants ATM-0753451 and ANT-0638587.

We thank the Cluster FGM, CIS, RAPID and EFW instrument teams, as well as the Cluster Active Archive for access to the data.

Topical Editor R. Nakamura thanks M. Volwerk and another anonymous referee for their help in evaluating this paper.

## References

- Baker D. N., Stauning, P., Hones Jr., E. W., Higbie, P. R., and Belian, R. D.: Near equatorial, high-resolution measurements of electron precipitation and  $L^*$ =6.6, *J. Geophys. Res.*, 86, 2295–2313, 1981.
- Baker, D. N., Peterson, W. K., Eriksson, S., et al.: Timing of magnetic reconnection initiation during a global magnetospheric substorm onset, *Geophys. Res. Lett.*, 29(24), 2190, doi:10.1029/2002GL015539, 2002.
- Baumjohann, W., Nagai, T., Petrukovich, A., Mukai, T., Yamamoto, T., and Kokubun, S.: Substorm signatures between 10 and 30 earth radii, *Adv. Space Res.*, 25(7–8), 1663–1666, 2000.
- Blake, J. B., Mueller-Mellin, R., Davies, J. A., Li, X., and Baker, D. N.: Global observations of energetic electrons around the time of a substorm on 27 August 2001, *J. Geophys. Res.*, 110, A06214, doi:10.1029/2004JA010971, 2005.
- Blake, J. B., Fennell, J. F., Friesen, L. M., et al.: CEPPAD – Comprehensive Energetic Particle and Pitch Angle Distribution Experiment on POLAR, *Space Sci. Rev.*, 71, 531–562, 1995.
- Hargreaves, J. K., Chivers, H. J. A., and Nielsen, E.: Properties of spike events in auroral radio absorption, *J. Geophys. Res.*, 84(A8), 4245–4250, 1979.
- Harvey, C.C.: Spatial Gradients and the Volumetric Tensor, in: *Analysis Methods for Multi-Spacecraft Data*, edited by: Paschmann, G. and Daly, P. W., ISSI Scientific Report SR-001 (Electronic edition 1.1), 2000.
- Henderson, M. G., Kepko, L., Spence, H. E., Connors, M., Sigwarth, J. B., Frank, L. A., Singer, H. J., and Yumoto, K.: The

- evolution of north-south aligned auroral forms into auroral torch structures: The generation of omega bands and ps6 pulsations via flow bursts, in: *Proceedings of the Sixth International Conference on Substorms*, edited by: Winglee, R. M., pp. 169–174, Univ. of Wash., Seattle, Washington, 2002.
- Kennel, C. F. and Petschek, H. E.: Limit on stably trapped particle fluxes, *J. Geophys. Res.*, 71, 1–28, 1966.
- Li, X., Sarris, T. E., Baker, D. N., Peterson, W. K., and Singer, H. J.: Simulation of energetic particle injections associated with a substorm on August 27, 2001, *Geophys. Res. Lett.*, 30(1), 1004, doi:10.1029/2002GL015967, 2003.
- Liang, J., Liu, W. W., Spanswick, E., and Donovan, E. F.: Azimuthal structures of substorm electron injection and their signatures in riometer observations, *J. Geophys. Res.*, 112, A09209, doi:10.1029/2007JA012354, 2007.
- Robert, P., Dunlop, M. W., Roux, A., and Chanteur, G.: Accuracy of Current Density Determination, in: *Analysis Methods for Multi-Spacecraft Data*, edited by: Paschmann, G. and Daly, P. W., ISSI Scientific Report SR-001 (Electronic edition 1.1), 2000.
- Spanswick, E., Donovan, E., Liu, W., Wallis, D., Aasnes, A., Hiebert, T., Jackel, B., and Henderson, M.: Substorm associated spikes in high energy particle precipitation, in *The Inner Magnetosphere: Physics and Modeling*, *Geophys. Monogr. Ser.*, vol. 155, edited by: Pulkkinen, T. I., Tsyganenko, N. A., and Friedel, R. H., p. 227, AGU, Washington, D.C., 2005.
- Spanswick, E., Donovan, E., Friedel, R., and Korth, A.: Ground based identification of dispersionless electron injections, *Geophys. Res. Lett.*, 34, L03101, doi:10.1029/2006GL028329, 2007.
- Wilken, B., Axford, W. I., Daglis, I., et al.: RAPID – The imaging energetic particle spectrometer on CLUSTER, *Space Sci. Rev.*, 79, 399–473, 1997.
- Zaharia, S., Cheng, C. Z., and Johnson, J. R.: Particle transport and energization associated with substorms, *J. Geophys. Res.*, 105(A8), 18741–18752, 2000.